ES Energy & Environment

DOI: https://dx.doi.org/10.30919/esee902

Layered Double Hydroxide (LDH) – MXene Nanocomposite for Electrocatalytic Water Splitting: Current Status and Perspective

Anandajayarajan Udayakumar,[1] Preethi Dhandapani,[1] Senthilkumar Ramasamy[2] and Subramania Angaiah[1,*]

Abstract

To address the need for clean and sustainable fuel sources, it is essential to develop a high-performance, low-cost and stable non-noble metal electrocatalyst for water splitting. Two-dimensional (2D) materials, namely Layered Double Hydroxide (LDH) and MXene, have recently gained popularity. Moreover, the combination of these two materials has been found to effectively address the issues related to poor conductivity, limited exposure of active sites, and small electrochemical active surface areas that hindered the practical application of LDH. In this review, we comprehensively evaluated the advancements made towards the development of MXene-based LDH hybrid nanomaterials for hydrogen evolution reaction (HER), oxygen evolution reaction (OER), and overall water splitting from both a theoretical and practical standpoint. Additionally, the review discusses various criteria used to assess electrocatalysts and the mechanism involved in the electrochemical splitting of water. Lastly, potential opportunities and future challenges of MXene-based LDH hybrids in hydrogen production through water splitting are examined.

Keywords: Layered Double Hydroxide; MXene; Hydrogen Production; Water splitting.
Received: 10 April 2023; Revised: 25 May 2023; Accepted: 25 May 2023.
Article type: Review article.

1. Introduction

The widespread usage of fossil fuels has caused severe environmental issues, which has led to an urgent need to investigate about clean, renewable and environmentally friendly energy sources.[1] In such cases, electrochemical water splitting serves as an effective and clean pathway for the production of hydrogen and oxygen. However, the usage of electrochemical water splitting on a large scale for commercial application is unfortunately constrained by the following three factors: (i) the need for a higher overpotential than the theoretical value (1.23 V) to run overall water splitting; (ii) the lack of stability of electrocatalyst materials; and (iii) the high price of electrocatalysts. The most common electrocatalysts utilized in industry to produce satisfactory performance in terms of hydrogen and oxygen productions are based on precious metals, also known as Platinum Group Metals (PGMs) (such as Pt, Pd, Ir, Ru and Rh).[2,3] However, the poor stability and expensive price of these noble metals prevent their wider application.[4-6] Several materials have been reviewed as electrocatalysts for water-splitting applications in the hunt for alternative and economically feasible electrocatalysts. These include metal and its alloys, transition metal oxides, hydroxides, chalcogenides, phosphides, borides, nitrides and carbides. Layered double hydroxides (LDH), a common type of hydroxide belonging to a family of two-dimensional materials, are unique among electrocatalysts due to their benefits, including low price, flexible structure, easy synthesis method, high surface area, distinct layered structure, and excellent catalytic activity in alkaline medium. This extensive group of compounds is often called hydrotalcites or anionic clays. The term "anionic clays" specifically highlights their complementary nature to cationic clays, which have interlamellar domains that contain cationic species.[7] LDH can be described by $[M^{2+}_{1-x}M^{3+}_{x}(OH)_2][A^{n-}_{x/n}\cdot mH_2O]$,[8] where M^{2+} stands for the divalent metal ions (Mg^{2+}, Zn^{2+},Ni^{2+}, Co^{2+}, Fe^{2+}, Cu^{2+})and M^{3+} stands for the trivalent metal ions (Al^{3+}, Cr^{3+}, Fe^{3+}, Mn^{3+},Ga^{3+}, In^{3+}) and A^{n-} corresponds to the anions[9-11] as shown in Fig. 1. LDH has many metal centers and wider interlayer spacing, resulting in outstanding electrocatalytic activity. Despite these advantages, their performance is still far from the best due to their weak conductivity and significant inclination to re-stack 2D nanosheets. In addition to that, the material has other

[1] *Electro-Materials Research Laboratory, Centre for Nanoscience and Technology, Pondicherry University, Puducherry, 605014, India.*
[2] *Department of Chemical Engineering and Materials Science, Amritha Vishwa Vidyapeetham, Coimbatore – 641112, India.*
**Email:* a.subramania@gmail.com (S. Angaiah)

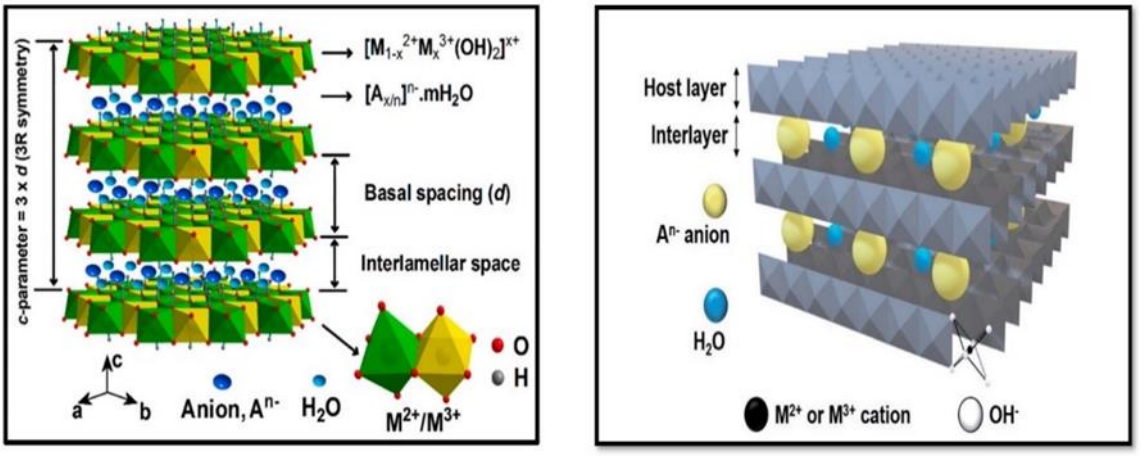

Fig. 1 Schematic representation of the classical LDH structure. Reproduced with the permission from [12,13], Copyright 2020 Applied Clay Science, and 2021 Journal of Materials Chemistry A.

shortcomings, including insufficient electrochemical active surface area (ECSA) and insufficient exposure of the active metal site.

Many research has been put forth to overcome these restrictions. For instance, the heterogeneous interfaces of the composite structure are regulated by (i) alloying with transition metal compounds, (ii) element doping,[14,15] (iii) introduction of defects[16-18] and (iv) coupling with a conductive substrate.[11] Among these, coupling with support material is considered advantageous because it shortens the charge transfer pathway in the catalyst by promoting better performance. Numerous support materials have been studied so far, including graphene, carbon nanotubes, rGO,[19] Mn_3O_4 nanoparticles, polypyrrole, and graphitic carbon nitrides (g-C_3N_4), carbon paper and transition metal nitrides or carbides. For example, Ming Gong *et al.* prepared nickel−iron layered double hydroxide (NiFe-LDH) nanoplates on mildly oxidized multiwalled carbon nanotubes (CNTs), which outperformed Ir in both activity and stability.[20]

Among various supports, a brand-new class of two-dimensional nanosheets called MXene is distinguished by its superior electrical conductivity, surface hydrophilicity, adjustable composition, and high chemical and mechanical stability. MXenes are represented as $M_{n+1}X_nT_x$, where M is early transition metals, X is a carbon (C), nitrogen (N), or both, n can take the values of 1, 2, 3 and T_x is the surface functional group. MXene can be produced by carefully removing the A layer from the MAX phase ($M_{n+1}AX_n$), where A corresponds to the group 13 and 14 elements. Further details about various methods of synthesis MXene are discussed later in this review. The coupling of LDH with MXenes results in several benefits such as enhanced electrical conductivity and prevention of restacking and aggregation, which results in the increased intrinsic activity of metal in LDH by creating a favourable environment in the electrolyte solution, which ultimately results in faster gas kinetics and rapid gas diffusion. Further, it creates additional active sites. Additionally, the LDH-MXene structure also provides more metal sites when exposed to the electrolyte, resulting in increased efficiency of the redox reaction and enabling a faster redox reaction.

Furthermore, the mechanical stability of the catalyst and its corrosion resistance in the electrolyte solution determine its stability. MXene can inhibit the corrosion of catalyst materials, and when used as support, it can provide mechanical stability to the catalyst. LDH-MXene is an emerging material with a bright future in energy conversion technology.[21] Jin Wang *et al.* reported that the synergetic effect between the LDH-MXene hybrid material NiFe-LDH/N_{10}TC/NF would effectively prevent electron/hole (e^-/h^+) recombination.[22] However, the utilization of MXene-based LDH hybrid electrocatalysts is still in the early stages. This review, for the first time, elucidate the application of LDH-MXene in various electrocatalytic water splitting application such as Hydrogen evolution reaction, Oxygen evolution reaction and overall water splitting. Besides that, the basics of electrocatalytic water splitting and analyzing criteria are emphasized.

2. Fundamentals of water splitting

The overall water splitting is a reasonably simple chemical process, with the following equation: $2H_2O \rightarrow 2H_2 + O_2$, where OER and HER occurs at the anode and cathode, respectively. The minimum energy needed for this process is 237.2 kJ mol^{-1} at 25 °C and 1 atm, with a voltage of 1.23 V.[23] However, in practice, a higher voltage is needed due to factors such as bubble resistance, activation energy, and hindrance to electrolyte diffusion.[24]

2.1 Hydrogen Evolution Reaction (HER)

The hydrogen evolution reaction (HER) is a complicated process with multiple-step that occurs on the surface of the cathode.[25] The initial step, known as the Volmer reaction, consists of the transfer of an electron to the electrode and the adsorption of a proton to form an absorbed hydrogen atom. This atom can then undergo two pathways to produce H_2. In the Heyrovsky reaction, another electron and proton are transferred from the solution to the absorbed hydrogen atom.

Alternatively, in the Tafel or combination reaction, two absorbed hydrogen atoms combine on the electrode surface to form H_2.[26,27] The HER reaction proceeds as follows.[28]

1. Volmer step (electrochemical adsorption):

In alkaline medium: $* + H_2O + e^- \rightarrow * H + OH^-$

In acidic medium: $* + H_3O^+ + e^- \rightarrow * H + H_2O$

2. Heyrovsky step (electrochemical desorption):

In alkaline medium: $* H + H_2O + e^- \rightarrow H_2 + OH^- + *$

In acidic medium: $* H + H_3O^+ + e^- \rightarrow * + H_2 + H_2O$

3. Tafel step (chemical desorption):

$2 * H \rightarrow H_2 + *$

where (*) represents active sites.

2.2 Oxygen evolution reaction (OER)

The electrocatalytic OER is a sophisticated four-step, four-electron oxidation process with three surface-adsorbed reaction intermediates: OOH*, O*, and OH*.[29] The OER has sluggish kinetics and necessitates a higher overpotential than the HER. Under acidic and alkaline circumstances,[28] the reactions at the cathode and anode sections of the water-splitting reaction are different and depicted in Fig. 2.[28]

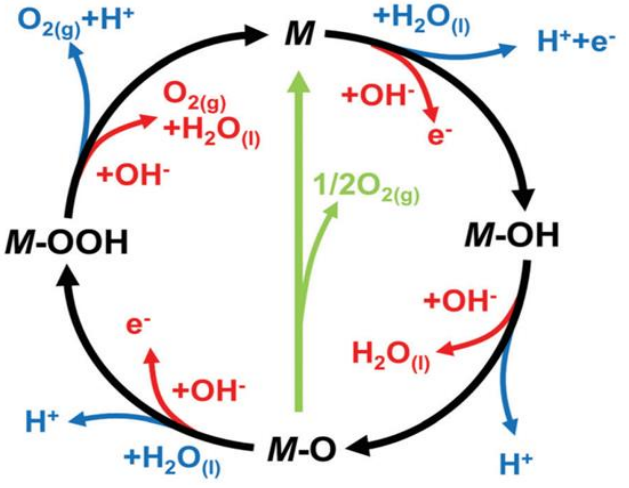

Fig. 2 The OER process is represented by a blue line for acidic conditions and a red line for alkaline conditions. Reproduced with the permission from [33] copyright 2017 Chemical Society Reviews.

Under basic conditions, the proposed reaction mechanism for the OER is stated as follows:[30,31]

$OH^- + * \rightarrow OH * +$

$OH * + OH^- \rightarrow O * + H_2O$

$2\ O * \rightarrow 2* + O_2$

$O * + OH^- \rightarrow OOH * + e^-$

$OOH* + OH^- \rightarrow * + O_2 + H_2O$

where * denotes the active site of catalyst, and OH*, O*, and OOH* are adsorbed intermediate species.

Under acidic conditions, the proposed reaction mechanism for the OER is described as follows:[32]

$* + H_2O \rightarrow OH* + H^+ + e^-$

$OH* + OH^- \rightarrow O* + H_2O + e^-$

$2\ O * \rightarrow 2* + O_2$

$O* + H_2O \rightarrow OOH * + H^+ + e^-$

$OOH * + H_2O \rightarrow * + O_2 + H^+ + e^-$

2.3. Evaluation parameters for electrocatalytic water splitting

Several parameters are used to evaluate electrocatalysts, such as onset potential, overpotential, Tafel slope, electrochemical active surface area, chronoamperometry, turnover frequency, and Faradaic efficiency. These parameters can be measured using either a three-electrode system or a two-electrode system, with the former containing a working electrode, reference electrode, and counter electrode. The catalyst of interest is loaded on the working electrode. In contrast, the reference electrode must be stable during the catalysis process and is typically chosen based on the pH condition. The counter electrode is used to complete the current circuit in the electrochemical cell. The two-electrode system does not include a separate reference electrode, with the counter electrode serving as the reference instead. This system may be preferred for reflecting the efficiency of the catalytic system as it more closely resembles real devices, which do not have a reference electrode.[33] It is worth noting that the reported values for these parameters may be influenced by the test conditions and methods, particularly the preparation of the working electrode. Fig. 3 represents the schematic representation for the evaluation of electrocatalytic parameters.

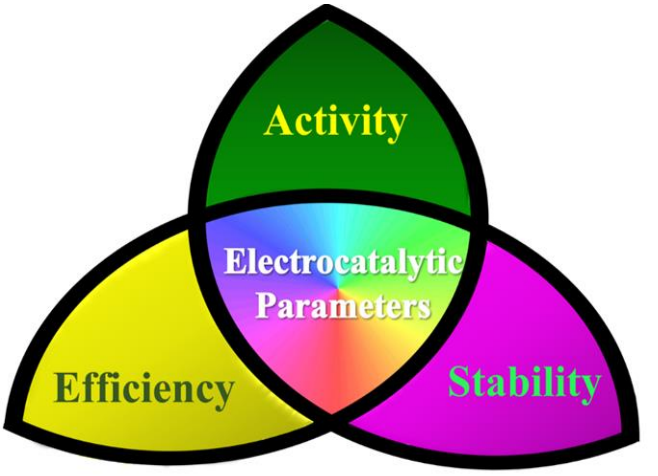

Fig. 3 Schematic representation for the evaluation of electrocatalytic parameters.

2.3.1 Overpotential (η)

Overpotential is one of the important criteria for analyzing electrocatalytic activity. The thermodynamic voltage of water splitting is 1.23 V at 25 °C and 1 atm, regardless of the medium in which it occurs. To perform electrochemical water splitting, we must utilize a voltage greater than the thermodynamic potential. The additional potential (known as Overpotential) is primarily employed to overcome intrinsic activation barriers on both the anode (a) and cathode (c), as well as other resistances (other), such as solution resistance and contact resistance.[34] Overpotential is defined as the difference

between the actual potential and the thermodynamic value under equilibrium conditions at a particular current density. Overpotential can be calculated by[35]

$\eta = E_{applied} - E_0 - iR$

where $E_{applied}$ is the actual applied potential, E_0 is the theoretical equilibrium value (E_0 = 1.23 V), and iR is the ohmic potential drop of the current flow. As can be seen from this equation, lowering overpotentials via appropriate approaches is essential in making the water-splitting process more effective. In the case of overall water splitting, two components are involved namely ηc and η, which represent overpotential associated with cathode and anode, respectively, as shown in Fig. 4. Therefore, researchers are striving to reduce the overpotential on both electrodes. The water splitting activity can be generally evaluated by Linear Sweep Voltammetry (LSV).[36] To quantify the electrocatalytic activity of a catalyst, the overpotential is measured at a current density of 10 mA cm^{-2}.[37] In summary, a promising electrocatalyst should be able to generate a higher current density while having a lower overpotential.[38-40]

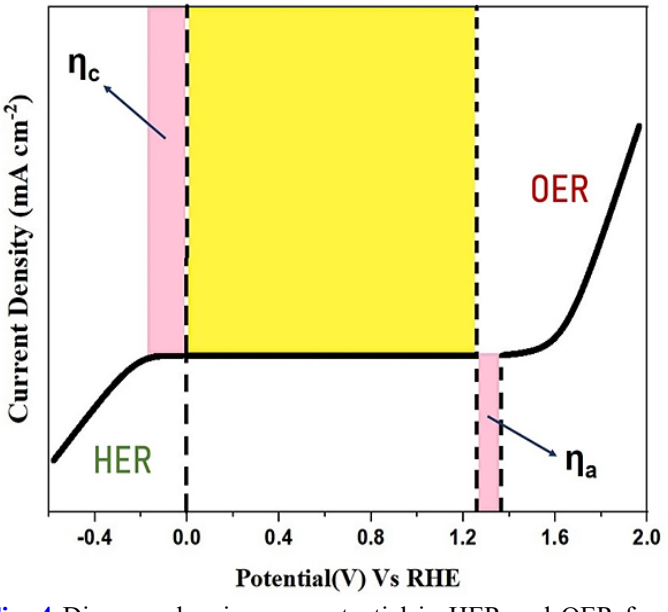

Fig. 4 Diagram showing overpotential in HER and OER from Linear Sweep Voltammetry.

2.3.2. Tafel slope and Exchange current density

Converting the current density from an LSV polarisation curve into a logarithmic scale (base 10) on the x-axis and the Overpotential on the y-axis results in a Tafel plot. The Tafel slope and Exchange current are the important factors used to evaluate activity. The following equation states the relationship between Overpotential and the logarithm of the current density (log j) α_c.[36,41]

$\eta = a + b \log j$

where η represents the Overpotential, b is the Tafel slope, j indicates the current density, and a is a constant. The Tafel slope is a critical kinetic parameter in electrochemical water splitting, indicating how fast the current density increases as the overpotential increases. It also aids in identifying the rate-determining step. Tafel slope is illustrated using the following equation:[42]

$$\frac{d\,log(j)}{d\eta} = \frac{2.303RT}{\alpha nF}$$

Where j denotes the current density, η is Overpotential, α is the charge transfer coefficient, and the number of electrons transferred during the electrochemical reaction is n.[43] For OER, n = 4 and for HER, n = 2.

A smaller Tafel slope means less overpotential is required to obtain the same current density, indicating quicker electron transfer kinetics. When η = 0, the corresponding current density is called the exchange current density (j_0), representing a further essential kinetic parameter of the electrochemical reaction rate at equilibrium.

2.3.3 Turnover frequency (TOF)

Another indicator of intrinsic activity is turnover frequency (TOF). It is defined as the number of desired resultants produced per second per catalytic site. In basic terms, TOF is the measure of the number of reactants that can be converted to the required product per catalytic site in a given amount of time. The TOF value can be determined using the following formula:[44-50]

$$TOF = \frac{jA}{\alpha nF}$$

where j (mA cm^{-2}) denotes the current density at a specific overpotential during the LSV measurement, the surface area of the working electrode is represented by the letter A, α is the electron number of the electrocatalyst, F (96500 C mol^{-1}) is the Faraday constant and n represents the molar amount of electrocatalyst which is calculated with the help of electrochemically active surface area (ECSA). Unfortunately, most heterogeneous electrocatalysts make it challenging to calculate the correct TOF value because the actual number of active sites per electrode area frequently approximates. Despite its limitations, TOF is a valuable tool for comparing the catalytic activity of different catalysts, particularly within the same system or under similar conditions.

2.3.4 Stability

Assessing stability is an essential factor to consider when exploring the electrocatalyst for practical applications. Two approaches can be utilized to evaluate stability: the cyclic voltammetry (CV) and the chronoamperometry (CA) or chronopotentiometry (CP) methods. (i) The cyclic voltammetry method compares the changes in overpotential before and after a definitive number of potential cycling runs (*e.g.*, 10,000 runs). A slight change in overpotential following several potential cycling suggests that the electrocatalyst endows stable. (ii) chronoamperometry (CA), or chronopotentiometry (CP) approach involves monitoring the potential (or current density) over time at a constant current density (or overpotential) of the electrocatalyst. For this method, the applied current density should not be less than 10 mA cm^{-2}, and the duration should be a minimum of 10 hours. If the potential or current remains the same over an extended

period, it indicates good stability.[23]

In addition to these methods, the stability or durability of the electrocatalyst can also be evaluated by comparing the LSV curves of the first cycle to those of the 1000th cycle after continuous cycling at a faster rate. An electrocatalyst with excellent stability showed a low shift in potential at a specific current density, as shown Fig. 5.

The structural and electrochemical stability of the electrocatalyst can also be assessed by comparing phase, elemental composition, and morphology before and after many cycles of cyclic voltammetry using techniques XRD, XPS, SEM, and TEM.[51,52] Fig. 5 shows the various stability tests.

2.3.5 Faradaic efficiency

Faradaic efficiency is an important index that describes the efficiency of electron utilization during the catalyzing reaction. In an electrocatalytic reaction, by definition, Faradaic efficiency is the ratio of the experimentally produced quantity of H_2 or O_2 to the theoretically calculated amount of H_2 or O_2. The theoretical values can be derived using the chronoamperometric or chronopotentiometry analysis.[53-55] The experimental values are determined by assessing gas production using either gas chromatography or water–gas displacement method. It is because of the rare side reaction water splitting has a high Faradic efficiency, which is beneficial to practical applications for energy usage efficiency. A higher faradaic efficiency indicates less energy loss during the electrochemical reaction.

2.3.6. Mass activity

The mass activity (MA) of an electrocatalyst is a metric used to assess its quality. It can be calculated by:

$$MA = {}^{j}/_{m}$$

where j represents the measured current density (mA cm^{-2}) and m denotes the mass of the electrode.

2.3.7 Electrochemical active surface area (ECSA)

The surface area of a catalyst is a vital factor, as it is critical in providing detail about the number of active sites available. The specific surface area of a porous catalyst is often measured by employing the Brunauer-Emmett-Teller (BET) N_2-adsorption technique. Still, it should be noted that this method may not be a precise way to evaluate the electrochemical surface area, which is better evaluated using electrochemical techniques. The BET specific surface area includes the whole surface; therefore, it is recommended to use the electrochemical surface area (ECSA) to evaluate the surface area of an electrocatalyst. Although it is currently challenging to obtain an accurate ECSA for an electrocatalyst, an approach that has been widely employed to evaluate the relative electrochemical surface area is based on the electrochemical double-layer capacitance (C_{dl}), which can be calculated from cyclic voltammetry (CV) curves in a specific potential window without Faradaic processes. A larger C_{dl} value indicates a higher surface area and more exposed surface reactive sites.

Measuring the ECSA allows researchers to compare the specific catalytic activity of various catalyst materials and investigate the degradation of the catalyst used under various circumstances and electrode configurations.[39,40] The formula is used to determine the ECSA is as follows:

$$ECSA = C_{dl} / C_s$$

3. Theoretical calculations

These performance assessment metrics may not always give an accurate representation. For example, the Tafel equation is used to uncover the mechanism and rate-determining step of the electrochemical process. However, there are often significant uncertainties in interpreting the complex reactions happening on the electrode surface.[56] Therefore, combining theoretical and experimental approaches is imperative to clarify the relationship between structure and activity.[57] Mohamed Benchakar *et al.* employed a combination of TEM-EELS and DFT calculations to examine the interface of the Co-LHD@$Ti_3C_2T_x$ composite. EELS results indicated that the defects formed on MXene had a beneficial effect on the composite material by providing a point of attachment for the catalyst. DFT calculations supported these findings, demonstrating that the change in interfacial chemistry is due to the deposition of Co-LDH on MXene.[58] Deng *et al.* have

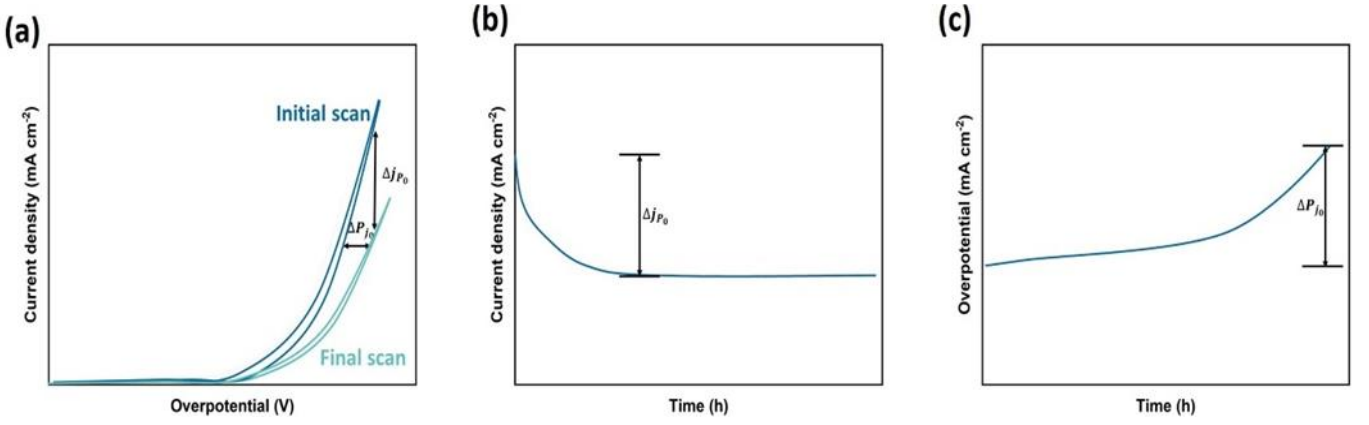

Fig. 5 Schematic diagrams for the evaluation of OER stability by (a) CV, (b) CA, and (c) CP. Reproduced with the permission from [52] Copyright 2022 Journal of Energy Chemistry.

used the density functional theory to examine the relationship between MXene and CoFe-LDH by calculating the density of states (DOS) for CoFe-LDH, MXene, and a composite of both materials. They found that the DOS of MXene near the Fermi energy level is lower than that of the composite material, suggesting that the combination of the two materials could improve electron conductivity (Fig. 6). This conclusion is supported by electrical impedance spectroscopy and conductivity tests. The improved conductivity is attributed to the formation of an area with a high concentration of electrons on MXene and an area with a high concentration of holes on CoFe-LDH, which caused a shift in the Fermi level.[59]

Furthermore, Chongyan Hao *et al.* investigated the interface-coupled CoFe-LDH/MXene nanohybrid by combining XPS and DFT calculations. The findings of his research demonstrated that the enhanced positive charges in the Co and Fe centers are the consequence of a spontaneous charge transfer between the Co and Fe atoms in the CoFe-LDH to the anion. The estimated density of states for pure CoFe-LDH and CoFe-LDH/MXene is also investigated. (Fig. 7) The results showed that the CoFe-LDH has a band gap of about 1.65 eV (semi-conductor in nature), whereas the CoFe-LDH supported by MXene has metallic properties. In addition, the presence of localized holes on the oxygen atoms suggests the existence of unpaired electrons, which agrees with the proposed mechanism for oxygen evolution reactions.[61] The research indicated that the oxidized oxygen ions in the CoFe-LDH/MXene system acts as electrophilic centers during Oxygen Evolution Reaction (OER) and improved interfacial coupling between the CoFe-LDH and MXene contributes to the material's high catalytic performance in the OER process.

4. Methods for the synthesis of MXene, LDH, and MXene-LDH hybrid materials

4.1 Synthesis of LDH

Understanding the synthesis procedure used to construct LDH-MXene requires knowledge of how each material is produced individually. A variety of methods are in use to produce layered double hydroxide. Some of the well-known techniques among them are (i) the Co-precipitation method, (ii) the electrodeposition method, (iii) the hydrothermal method, (iv) the ion-exchange method, (v) microwave treatment method, (vi) the sol-gel method, and (vii) urea process.[10] Apart from these popular methods, other synthesis strategies have also been implemented to produce LDHs, such as the mechanochemical method (ball milling precursors), reconstruction method, electrospinning, electrostatic interstratification and micro-emulsion method.

4.1.1 Co-precipitation method

The co-precipitation method is a simple and popular procedure to synthesize LDH, which involves dissolving inorganic salts in an alkaline solution at a constant or increasing pH,[62] which is usually done with the help of sodium hydroxide, ammonium hydroxide, or urea. Controlling the pH is a crucial factor in the production of LDH, as a low pH value prevents all metallic

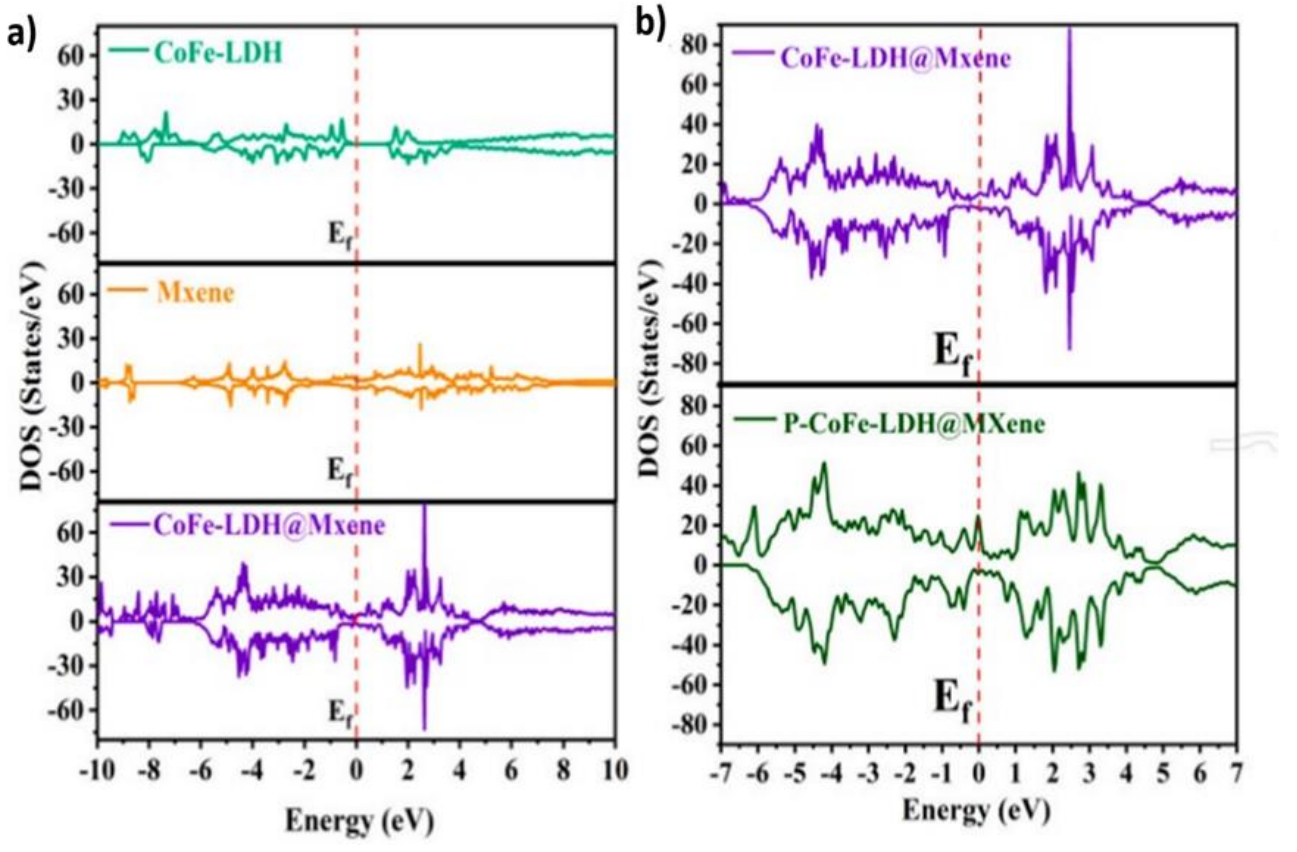

Fig. 6 Density of state of the a) CoFe-LDH, MXene, and CoFe-LDH@MXene b) CoFe-LDH@MXene and P-CoFe-LDH@MXene; Reproduced with the permission from [52], Copyright 2021 Applied Catalysis B: Environmental.

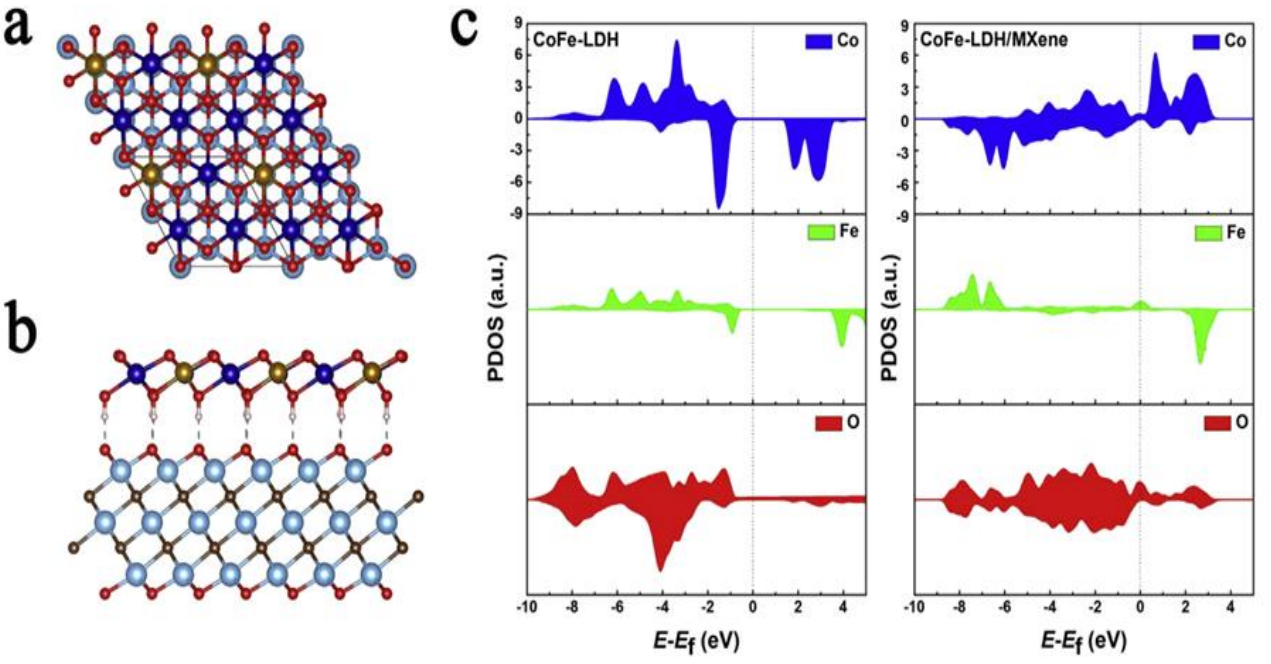

Fig. 7 (a) Top view and (b) side view of model structure of CoFe-LDH/MXene; (c) projected density of states (PDOS) of individual CoFe-LDH and CoFe-LDH/MXene. The Fermi level is shifted to zero. Reproduced with the permission from [60] copyright, 2021, Applied Catalysis B: Environmental.

ions from precipitating completely, and a very high pH value causes metallic ions to leach.[10] This process allows controlling the particles size of the resulting LDHs based on the solution's supersaturation. Feitknecht was the first to report the synthesis of LDHs by this method in 1942, using dilute solutions of the reactants to synthesize [Mg-Al-CO_3] LDHs. Subsequent research by Gastuche *et al.* in 1967.[63] and Miyata in 1975[64] and 1980[65] explored the impact of modifying various parameters, including reactant concentrations and washing conditions on the co-precipitation synthesis process.

4.1.2 Hydrothermal Treatment

On the other hand, the hydrothermal method uses elevated temperature and pressure to produce the desirable LDH. In this method, the precursors comprising metal ions and anions are blended with water (solvent), and this aqueous solution is subjected to high temperature and pressure within a Teflon-lined autoclave with various synthesis times[66-68] The three most often utilized metal ion source precursors are metal oxide, metal hydroxide, and metal nitrate[69,70]. In 2012, Liao *et al.* utilized natural brucite and $Al(OH)_3$ to investigate the morphological and structural characteristics of hydrotalcite produced over various conditions.[71] Better crystalline LDHs are produced with this technique.[12] Moreover, the hydrothermal method is mainly preferred for the growth of LDH over various supports such as Nickel foam, graphene, CNT and MXenes. Another popular technique for developing LDH is electrodeposition. This method uses a typical three-electrode setup, where the working electrode is a conductive substrate, and the electrolyte is an aqueous solution containing a metal precursor.[12] The main benefits of this method include (i) the ability to form the catalyst without the use of any additives directly on the conductive substrate and (ii) properties of the layers deposited can be changed by adjusting the synthesis parameters, such as the concentration of the electrolyte, the type of solvent used and the type of electrodeposition method employed.

4.1.3 Sol–gel method

The sol-gel method is widely utilized because it is affordable and produces high-quality compounds. The sol-gel process has the added benefit of allowing control over the uniformity and structural performance of the resulting solid, at the preparation stage by adjusting the composition of precursors, synthesis temperature, reaction time, and the inclusion or exclusion of reactant species.[10] This technique involves dissolving the desired metal sources, which may be inorganic salts or metal-organic compounds, in water at 35ºC. Recently, high-purity LDH materials synthesized through the sol-gel method have been considered as potential photo(electro-)catalysts. For example, Prince *et al.* synthesized MgAl-LDH, NiCoAl-LDH, and NiAl-LDH thin films using the sol-gel method.[72] Similarly, Ahmed *et al.* prepared Mg/Fe-LDH using CTAB as pore directing and structural agent.[73]

4.2 Synthesis of MXene

There are two main categories of MXene synthesis namely Bottom Up and Top-Down approach. Top-Down is a method that breaks down large bulk materials into tiny nanoparticles. The fundamental mechanism behind this method involves

breaking of the more vital, weaker M-A link, while maintaining the M-X bond, by effectively removing the A layer from the MAX phase (transforming from a solid and dense state into a loosely packaged melodeon-like structure) similar to exfoliated graphite.[74]

There are several types of top-down methodology. Among these, the most well-known are the fluorine-containing acid etching technique, the molten fluoride salt etching, alkali etching, and electrochemical etching; these techniques are often referred to as liquid phase etching. The most often utilized etchant in the fluorine-containing acid etching technique is aqueous hydrofluoric acid (HF). The first synthesis of Ti_3C_2 MXene is via HF etching, where the A layer of the MAX phase is selectively etched.[75] By using HF etching, numerous members of the MXene family have been successfully created so far. Due to the hazardous nature of HF, alternative methods have been developed, including a modified acid etching technique[76] that combines HCl with fluoride salts such as LiF, NaF, KF, NH_4F, and FeF_3 to limit the use of HF. However, the inability of acid etchant to produce nitride-based MXenes has necessitated molten salt synthesis. As a result, MXenes can be produced by selectively etching using eutectic molten fluoride salt (KF + LiF + NaF). These fluoride-based etchants further increase the concerns regarding the environmental impact. Alkaline etchants are therefore viewed as environmentally beneficial and effective. This technique employs a high concentration of sodium hydroxide as an etchant. In the bottom-up approach, fundamental units are assembled into more complex structures. This technique allows, MXenes to grow directly on a desirable substrate. Chemical vapour deposition is a widespread technique (CVD), which involves placing the substrate and raw materials in a reaction chamber and setting reaction parameters. The primary benefit of this approach is that it yields high-quality MXenes.

Only a fraction of the techniques mentioned above were used in the synthesis of LDH-MXENE, and the procedure involved in this synthesis is the combination of MXene synthesis techniques and synthesis methods of LDHs.

4.3 Synthesis of LDH-MXene

Xuemei Li *et al.* prepared NiCo-LDH/$Ti_3C_2T_x$/NF hybrid for OER application by a two-step process, where first $Ti_3C_2T_x$ was prepared by HF etching followed by a hydrothermal technique in which NiCo-LDH is allowed to grow over Mxene.[77] Yi Liu *et al.* successfully synthesized 2D/2D NiMn-LDHs/Ti_3C_2-MXene hybrid by separately preparing Ti_3C_2 MXene using the mixed solution of LiF + HCl as the etchant, followed by the hydrothermal reaction for growing NiMn-LDH over Ti_3C_2 Mxene.[78] Mengzhou Yu *et al.* demonstrated the fabrication of Lanthanum doped NiFe-LDH onto vertically oriented MXene by electrodeposition technique, where the MXene is synthesized by an etching approach employing LiF + HCl as the etchant, which displayed excellent high current density performance. Similarly, Jin Wang *et al.* synthesized NiFe-LDH/N_{10}TC/NF electrocatalyst for a water splitting system, where the modified acid etching was employed for synthesizing MXene, over which NiFe-LDH material is electrodeposited.[22] Unlike them, Yangyang Wen *et al.* constructed a hybrid of Cerium doped NiFe-LDH built over $Ti_3C_2T_x$ MXene by in-situ co-precipitation method as shown in Fig 8(b), where they also etched out $Ti_3C_2T_x$ MXene from Ti_3AlC_2 MAX phase using a mixture of lithium fluoride and hydrochloric acid.[8] Similarly, Chongyan Hao *et al.* selectively etched Al from the MAX phase and carried out in-situ growth by coprecipitation of Fe^{3+} and Co^{2+} in as-prepared Ti_3C_2 MXene forming CoFe-LDH/Mxene,[60] as shown in Fig. 8(a).

5. LDH-MXene based electrocatalysts for water splitting

In recent days, layered double hydroxide (LDH)-MXene hybrids have gained much attention as electrocatalysts for water splitting due to their appealing characteristics, such as a short charge transfer pathway, enhanced conductivity, rapid mass transport and enhanced structural stability.

5.1 HER electrocatalyst

There has been significant research into Ni-Fe LDH materials due to their exceptional water-splitting performance. However, their semiconducting features and high surface energy have limited their usage in water-splitting systems, as they have limited electron conductivity and a tendency to agglomerate.[79] To address these issues, Ni-Fe LDH materials can be integrated into support materials with better conductivity and surface area.[22,80] MXenes, known for their layered structure, metallic conductivity, high hydrophilicity, and better surface chemistry, provide new opportunities for creating hybrid electrocatalysts on diverse supports.

Binfeng Shen *et al.*, through a hydrothermal co-assembly process, encased the $Ti_3C_2T_x$ MXene-RGO network within Ni-Fe LDH nanosheets. The as-prepared hybrid electrocatalyst possessed distinct textural advantages, particularly sizeable specific surface area, ultrathin walls, consecutive meso– and macroporous structure, evenly-distributed LDH layers, optimized electronic structure, and much charge-transfer pathways. On application, the LDH/MX-RGO hybrid exhibited a minimal onset electrode potential of merely 162 mV in 1 M KOH solution. Surprisingly, this hybrid electrode needed 326 mV and 524 mV overpotentials to generate 10 and 100 mA cm-2, current densities, respectively. It has a larger electrochemical active area and a lower charge transfer resistance than other control samples. The Tafel slope was as low as 100 mV dec^{-1} and maintained long-term stability as the current density of the electrocatalyst remained almost unchanged after 40 hours, as shown in Fig. 9. Further, LDH/MX-RGO electrode still has a comparable polarisation curve with almost no HER current loss, confirming its dependable electrocatalytic durability. The exceptional performance of this hybrid is believed to be due to the optimum LDH content, which can maintain the discrepancies

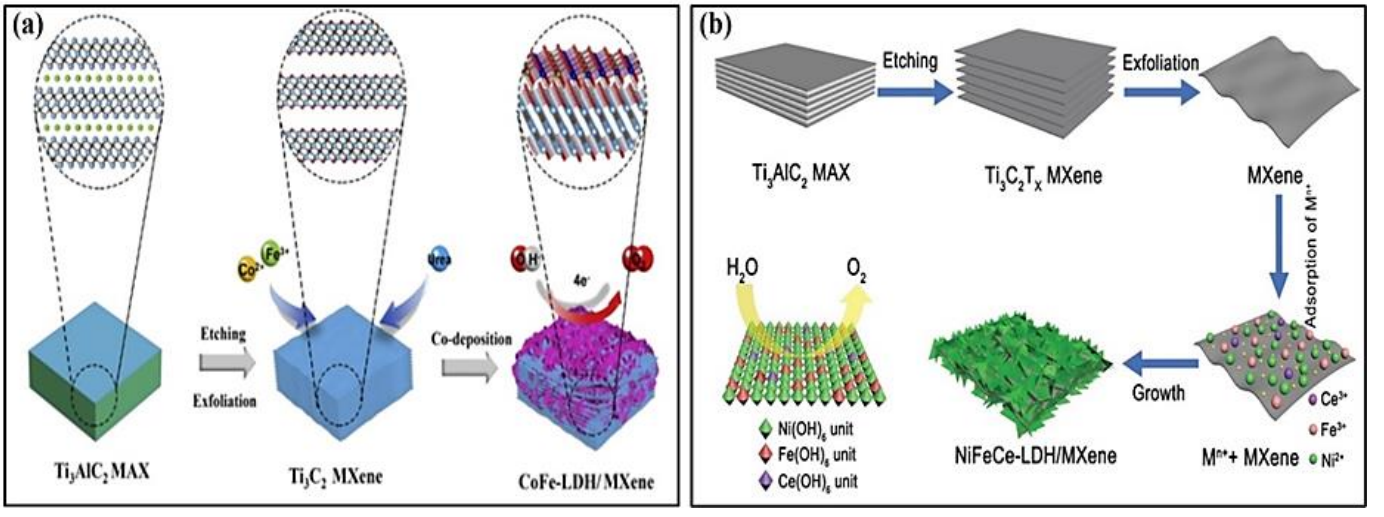

Fig. 8 Synthesis of (a) CoFe-LDH/MXene nanohybrid and (b) NiFeCe-LDH/MXene hybrid. Reproduced with the permission from [60], Copyright 2019 Materials Today Energy.

between the number of active sites and electron conductivity, thereby matching the synergistic coupling effects.[81]

5.2 OER electrocatalyst

Despite the high catalytic activity, LDH has limitations such as low conductivity and a tendency to agglomerate. These issues can be addressed by using MXenes as a support for LDH, which helps to prevent agglomeration and boosts activity. In addition, incorporating graphene can improve the poor conductivity of LDH. Capitalizing on these facts, Zuolei Zhu *et al.* synthesized NiFe LDH/$Ti_3C_2T_x$-rGO using a series of chemical methods and evaluated its OER performance in alkaline media. At 10 mA cm^{-2}, the resultant electrocatalyst has a 235 mV overpotential and a modest Tafel slope of 40 mV dec^{-1}. This enhanced electrocatalytic activity is believed to be due to Mxene, which reinforced charge transfer and generated more active sites. Electrochemical impedance spectroscopy (EIS) studies revealed an R_{ct} of 4.2 Ω, indicating improved charge transport kinetics. Furthermore, NiFe LDH/$Ti_3C_2T_x$-rGO showed good stability, with only a slight potential decrease after 12 hours of testing at a current density of 10 mA cm^{-2} .[82]

In addition, it is also common practice to coat the prepared electrocatalysts onto a conductive substrate, such as glassy carbon and carbon cloth, with the help of adhesives like Nafion or polyvinylidene fluoride, which ultimately limits its catalytic activity. To address this issue, Xuemei Li *et al.*, utilizing a two-step methodology, synthesized NiCo-LDH/$Ti_3C_2T_x$/NF by taking advantage of the three-dimensional structure of nickel foam. Furthermore, this as-prepared catalyst with flower-like morphology provided more edge sites because of its large surface area.[77] Furthermore, even at a high current density of 100 mA cm^{-2}, it needed a small overpotential of 223 mV and a Tafel slope of 47.2 mV dec^{-1}. Thus, the enhanced double layer capacitance value of 8.58 mF cm^{-2} indicates that more active sites are exposed, making them more available for catalytic activity.

Similarly, Zhichao Li *et al.* created an electrode of NiFe LDH/$Ti_3C_2T_x$/NF by electrodeposition method, combining the advantages of $Ti_3C_2T_x$, which has high electronic conductivity with the high electrochemical activity of NiFe LDH, allowing it to take the advantages of unique qualities of both materials. This as-prepared electrocatalyst demanded an overpotential of 200 mV at a current density of 10 mA cm^{-2}. This lower overpotential is attributed to the favourable heterostructure between MXene and NiFe-LDH for OER. It also exhibited good kinetics, which can be identified from a lower R_{ct} value obtained from EIS and a lower Tafel slope value of 64.2 mV dec^{-1}. In addition, stability tests of various forms are analyzed, including chronopotentiometry, cyclic voltammetry, linear sweep voltammetry and SEM and XPS before and after. The developed electrocatalyst is stable for 24h at a current density of 10 mA cm^{-2} in chronopotentiometry and sustained cyclic voltammetry for 5000 cycles, and no deformation is observed in structure and composition after the stability test, which is further analyzed using SEM and XPS, indicating the enhanced stability.[83]

In recent years, various strategies have been developed to address issues of LDH-based materials, such as the lessening of active sites and the restacking issue. However, this can be overcome by using a template for synthesizing LDH. Metal oxides, supramolecular structures, and metal-organic frameworks (MOF) are a few examples of standard templates. Capitalizing on this information, Liuyong Hu *et al.* prepared CoFe MLDH/Ti_3C_2/NF through an etching-doping procedure. This as-synthesized catalyst possessed considerably low overpotentials 170 and 238 mV to reach 10 and 100 mA cm^{-2}. The lower Tafel slope value of 31.5 mV dec^{-1} indicates improved OER kinetics.[84]

Additionally, this catalyst attained a Faradaic efficiency of 96%, indicating that no by-products are formed. The high TOF value of 0.68 s^{-1} showed superior intrinsic activity of the catalyst. Typically, a standard current density of 10 mA cm^{-2} is used to assess the electrocatalytic stability. However, high

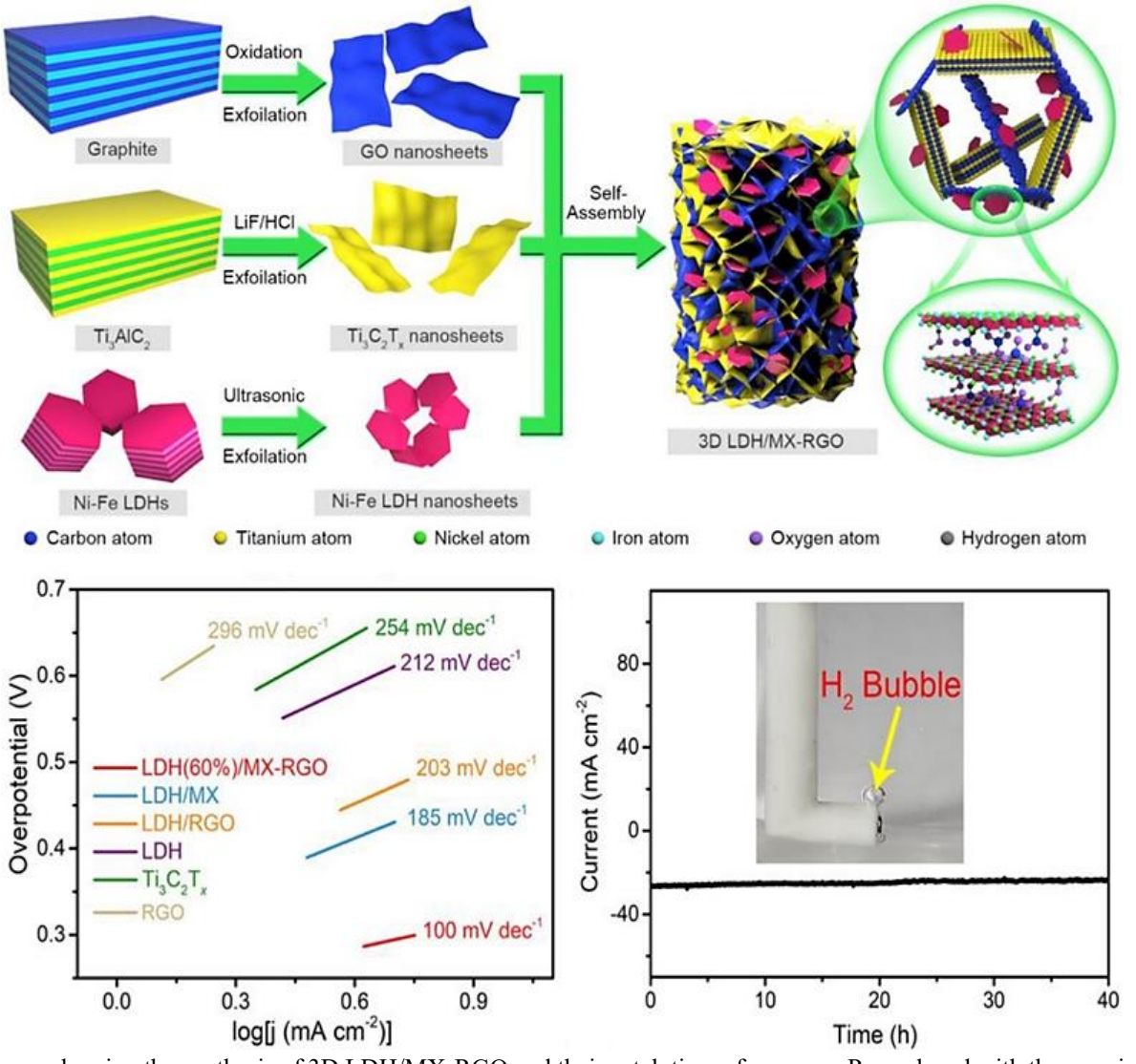

Fig. 9 Diagram showing the synthesis of 3D LDH/MX-RGO and their catalytic performances Reproduced with the permission from [81], Copyright 2022 Electrochimica Acta.

current density, such as 50 mA cm $^{-2}$, is unavoidably required to demonstrate a potential for use in practical applications. The CoFe MLDH/Ti_3C_2/NF was sustained for a time period of 50 h without the decline in current density. Further, the XPS results of the catalyst after the stability test are compared to those before the test, demonstrating superior stability.

Mengzhou Yu *et al.* prepared a nanohybrid electrocatalyst by synergistically coupling FeNi LDH nanoplates with Ti_3C_2 MXene nanosheets (named FeNi-LDH/Ti_3C_2-MXene), as depicted in Fig. 10. The FeNi-LDH/Ti_3C_2-MXene catalyst remained stable for 12 h in chronoamperometry testing. To further enhance its stability, this catalyst is supported with nickel foam (NF) which results in significant increase in stability. The FeNi-LDH/Ti_3C_2-MXene/NF catalyst maintained a constant potential of 1.53 V for 60 hours. Further, this catalyst exhibited a low Tafel slope of 48 mV dec^{-1}, showing enhanced kinetics. This progress in stability, activity and kinetics is due to robust interfacial interactions, facilitated electron coupling, and enabled rapid charge transfer at the interface of FeNi-LDH and Ti_3C_2 MXene. Further, the improved electronic interaction was confirmed by analyzing the UV–vis spectrum and XPS.[85]

5.3 Overall Water Splitting Electrocatalysts

Layered double hydroxides as an electrocatalyst face significant challenges in the case of mass production. The major hindrance is a lack of catalytic activity in bulk, which hinders sufficient active metal ions from being exposed in the bulk phases. Moreover, its low electron conductivity and insufficient electrochemical active surface area remain the central issue. The prime strategy to boost the catalytic performance by shortening the charge transfer channel in the catalyst is to connect the LDH with conductive support, which addressed the problem mentioned earlier to a significant degree. Among all classes of materials (graphene, carbon paper, reduced graphene oxides (rGO), carbon nanotubes, CNT *etc.*), highly conductive MXene structures provide the best performance due to their hydrophilic surface, excellent conductivity, high chemical and mechanical stability and rich surface chemistries. By improving the water adsorption and

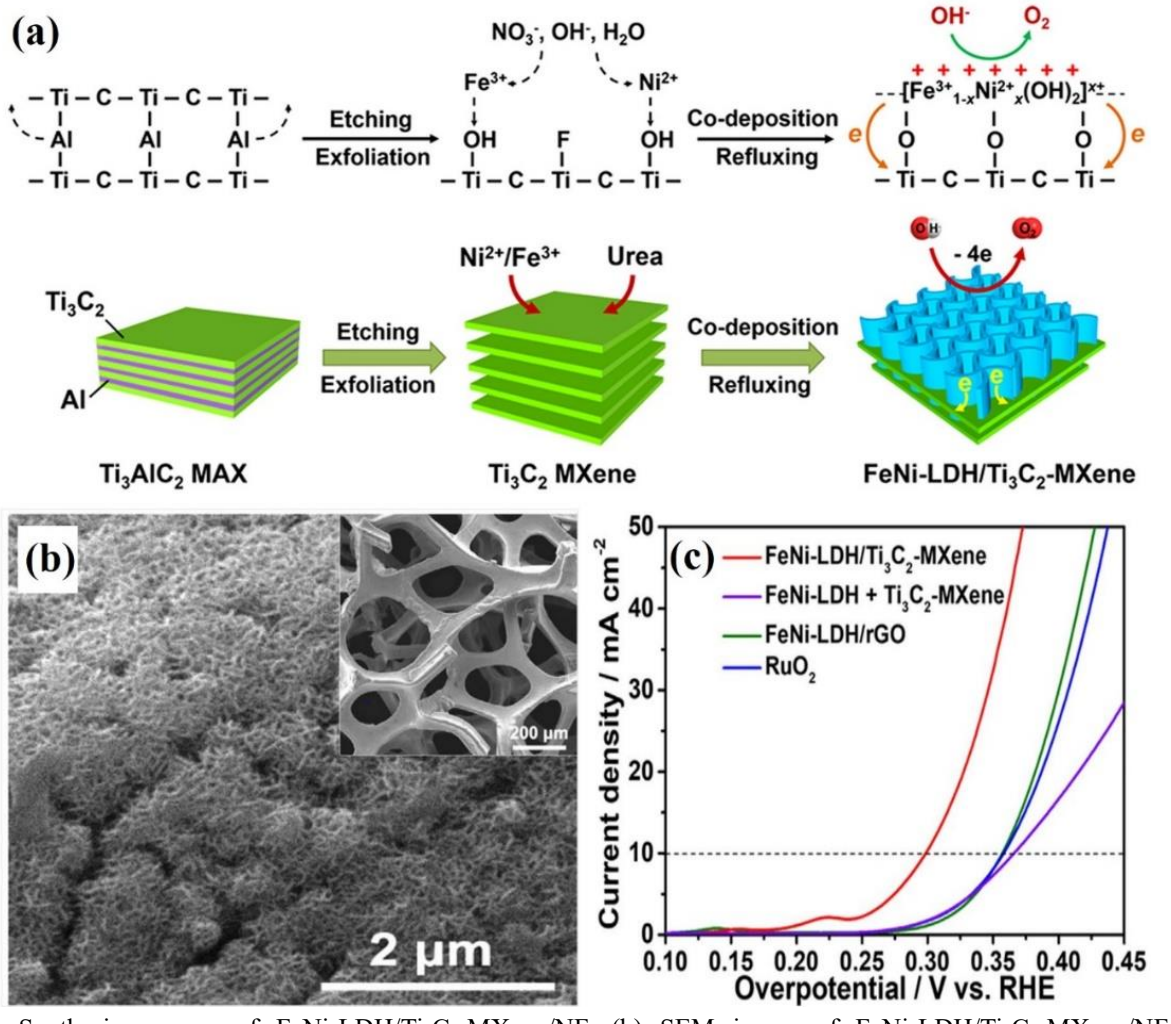

Fig. 10 (a) Synthesis process of FeNi-LDH/Ti_3C_2-MXene/NF, (b) SEM image of FeNi-LDH/Ti_3C_2-MXene/NF and (c) Electrocatalytic performance of FeNi-LDH/Ti_3C_2-MXene/NF Reprinted with the permission from [85], Copyright 2018 Nano Energy.

activation of the catalyst, MXene increases the conductance of LDH, stimulates the transfer of charge over the catalyst, and ramps up the Volmer step in the HER and OER redox process of the LDH. The synergistic relationship between LDH and Mxene has recently attracted the attention of several groups. Mingjing Li *et al.* combined experimental and theoretical approaches to investigate the water-splitting performance of FeCo-layered double hydroxide and P-MoO_3 grown by in-situ technique on MXene. This as-prepared catalyst demonstrated remarkable catalytic activity for overall water splitting at a current 10 mA cm^{-2} with a small overpotential of 179 mV and 118 mV for OER and HER, respectively. Furthermore, their corresponding Tafel slopes are as small as 40.44 $mVdec^{-1}$ for OER and 105 mV dec^{-1} for HER, showing improved kinetic performance.[86] The prepared catalyst also showed better stability for 42 h, as shown in Fig. 11 and maintained a Faradaic efficiency of up to 96 %. The improved performance of the prepared electrocatalyst is attributed to (a) enhanced electrocatalytic activity caused by the MXene-LDH interface, which makes it easier for the catalyst to transfer mass and charge. (b) MXene speeds up the oxidation-reduction process of the Oxygen Evolution Reaction of LDHs and the Volmer step of the Hydrogen Evolution Reaction by improving the adsorption/activation of water over the catalyst and the synergistic chemical interaction with LDH. Meanwhile, MXene also boosts mechanical stability, resulting in the stability of said catalyst (c). According to DFT calculations, it is known that electrocatalysis efficiency is increased by altering the d-band center of the reaction site, which combinedly enhances the binding energies of reaction intermediates.

The basic mixing of MXene and LDH cannot fully capitalise the merits of LDH@MXene because of low mechanical stability and restriction on electron transmission at the non-ohmic interface of two different materials. To develop an effective OER electrocatalyst, it would be effective to grow LDH (low conductivity) directly onto MXene (high conductivity). Recently, Lequan Deng *et al.* found that the interface effect of the Schottky heterostructure between CoFe-hydroxide and MXene with phosphorus (P) doping provides a practical approach to solve the limitations such as synergistically exposing more active areas and optimizing the intrinsic activity leading to the enhancement of bifunctional performance of P-CoFe-LDH@MXene/NF. This hybrid

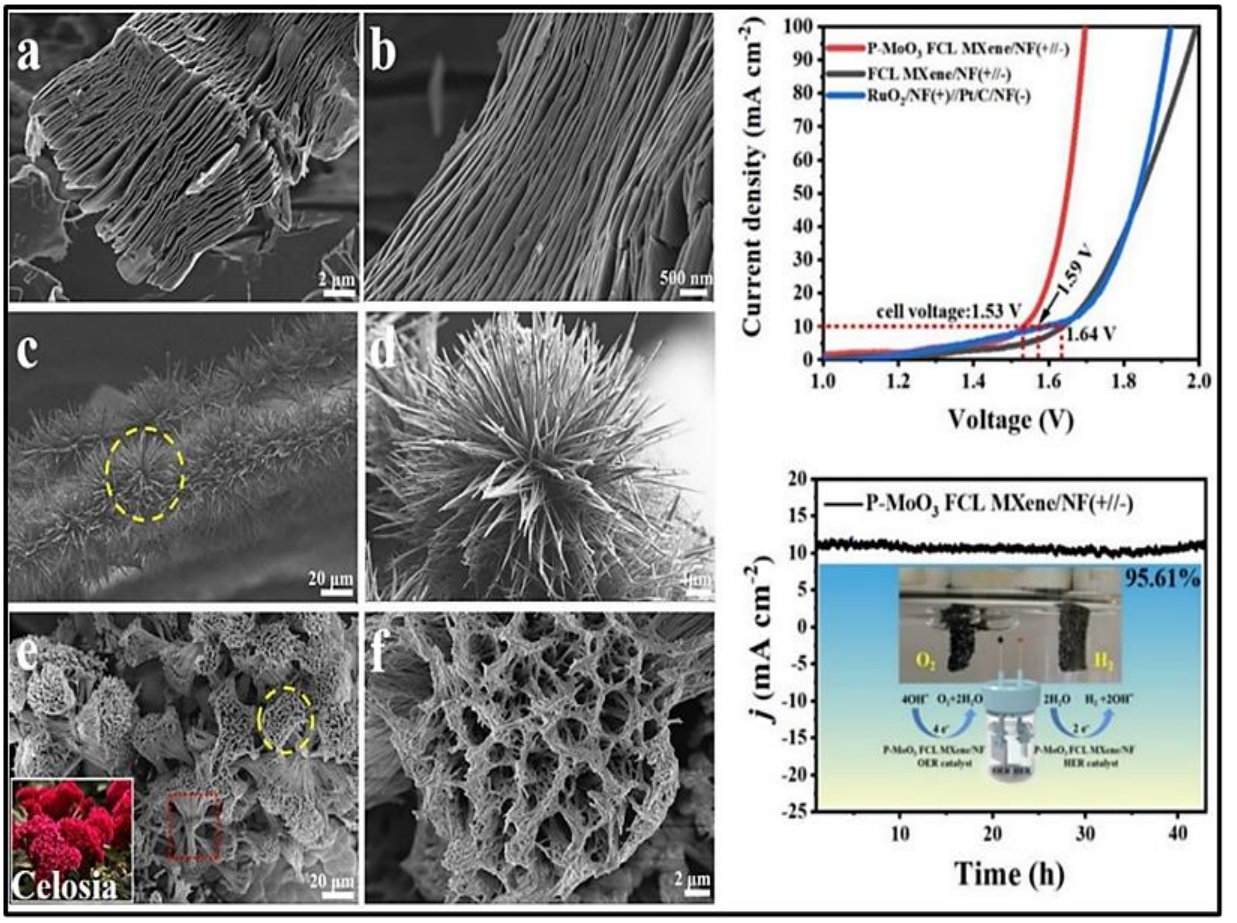

Fig. 11 FESEM images of (a,b) MXene, (c,d) FCL MXene/NF, (e,f) P-MoO_3 FCL MXene/NF, electrocatalytic performance and photo illustration of P-MoO_3 FCL MXene/NF. Reproduced with permission from [86], Copyright 2022 Chemical Engineering Journal.

Table 1. Summary of electrocatalytic performance of LDH@MXene based electrocatalysts.

Material	Overpotential (mV)		Cell Voltage (V)	Tafel Slope (mV dec^{-1})		Faradaic Efficiency (%)	Stability (hrs)	Ref.
	HER	OER		HER	OER			
LDH/MX-RGO	326	-	-	100	-	-	40	[81]
FePc-NiCo-LDH/Ti_3C_2	-	270	-	-	113.0	-	-	[88]
FeNi-LDH/Ti_3C_2-MXene	-	298	1.53	-	43.0	-	60	[85]
NiFe LDH/Ti_3C_2Tx-rGO	-	235	-	-	40.0	-	8.3	[82]
P-MoO_3 FCL MXene/NF	118	179	1.53	-	-	-	42	[86]
NiFeLa-LDH/v-MXene/NF	38	191	1.48	40	40.0	99%	400	[87]
FeCo-LDH/MXene hybrid	-	268	1.52	-	85.0	98 %	8.3	[89]
CoNi LDH/Ti_3C_2Tx MXene	-	257	-	-	68.0	98%	50	[89]
Co-LDH@MXene	-	330	-	-	82.0	-	-	[89]
NiCo-LDH/Ti_3C_2Tx/NF hybrid	-	223	-	-	47.2	-	12	[77]
NiMn- LDHs/Ti_3C_2-MXene	-	294	-	-	83.7	-	-	[78]
CoFe-LDH/MXene	-	319	-	-	50.0	-	10	[90]
$H_2PO_2^-$/FeNi-LDH-V_2C	-	250	-	-	46.5	96 %	13.8	[90]
CoFe MLDH/Ti_3C_2	-	170	1.41	-	31.5	96 %	50	[84]
NiFe-LDH/N_{10}TC/NF	-	264	-	-	58.1	99%	50	[22]
NiFeCe-LDH/MXene	-	260	-	-	42.8	-	20	[8]
FeNi-LDH/Ti_3C_2-MXene	-	300	-	-	48.0	94%	12	[91]
CoFe-LDH@MXene/NF	85	252	1.52	98.59	53.19	-	100	[59]
NiFeLDH/Ti_3C_2Tx/NF	-	200	-	-	64.2	-	24	[83]
NiCoFe-LDH/Ti_3C_2 MXene/NCNT	-	332	-	-	60.0	-	10	[92]

catalyst exhibited the lowest overpotential of 85 mV for HER at 10 mA cm^{-2} and 252 mV for OER at 200 mA cm^{-2} in an alkaline medium. The alkaline water electrolyzer required only 1.52 V voltage at 10 mA cm^{-2} for overall water splitting. Importantly, under acidic conditions, this electrocatalyst exhibited good long-term electrochemical stability for 100 h toward the HER and OER. Moreover, at 100 mA cm^{-2}, it retained stability for 100 hours with barely perceptible fluctuations under higher current density.[59]

Among the LDHs, NiFe-based LDHs are seen as potential electrocatalysts because of their availability and outstanding electrochemical performance. The strong synergistic interaction between the Fe and Ni metal centers and the favourable kinetics of unique layered structure enables NiFe-LDHs to exhibit outstanding OER activity, while their HER activity is frequently below average in alkaline electrolyzers. At the same time, the limited surface area brought by aggregation combined with the low conductivity of NiFe-LDH results in a significant overpotential. Mengzhou Yu *et al.* synergistically coupled La-doped NiFe-layered double hydroxides nanosheets and vertically aligned MXene nanosheets, abbreviated as NiFeLa-LDH/v-MXene/NF. The as-synthesized catalyst displayed significantly decreased overpotentials of 233 mV (HER) and 255 mV (OER) to achieve a high current density (500 mA cm^{-2}). The overall water electrolysis performance and durability of NiFeLa-LDH/v-MXene/NF were also excellent: 1.48 V cell voltage at 10 mA cm^{-2} and stable for a longer duration of 400 hours. The superior performance of NiFeLa-LDH/v-MXene/NF electrodes was attributed to the synergistic effect between La-doped NiFe-LDH and 3D vertically oriented MXene, which lowered charge transfer resistance and elevated instinct electrocatalytic activity as seen by a higher TOF number. Furthermore, the vertical alignment of MXene on the microporous structure of nickel foam improved the mass loading of the active material, which in turn increased the availability of electrochemically active sites and enlarged the ECSA.[87]

6. Conclusion and Perspective

The new 2D hybrid materials, "LDH-MXenes" have enormous potential for electrocatalysis, including HER, OER, and overall water splitting. The extensive research initiatives on developing hybrid electrocatalysts of layered double hydroxides with MXenes (LDH-MXenes) and their use in the electrochemical water splitting sector were presented systematically in this review for the first time. A particular focus is placed on various evaluation metrics and mechanisms underlying the water-splitting processes (HER & OER). The synthesis methods used to prepare LDH-MXene and its components are discussed in detail. It has been well-documented that every limitation of LDH as an electrocatalyst, such as its poor electrical conductivity, limited ECSA, inadequate exposure to active sites, and tendency to aggregation, can be overcome by coupling LDH and MXene. These include (1) inhibiting the development of clusters and preventing the formation of aggregates and (2) favoring an improvement in electrocatalytic performance by reducing the distance of mass diffusion and enhancing charge transfer. (3) The coupling also boosts the number of active sites, encouraging quick gas diffusion and increased efficiency.

Despite the critical acclaim received by LDH-MXenes-based electrocatalysts, several challenges still need to be addressed. The identified shortcomings are as follows: (i) While their stability is comparable to benchmark materials, their activity, particularly in terms of overpotential, significantly lags behind that of noble metals, (ii) Although they exhibit strong performance, further research is required to explore their feasibility for large-scale industrial applications, (iii) To gain a deeper understanding of the predominant synergistic effect within this material, it is essential to employ in-depth theoretical analysis and advanced spectroscopy techniques such as X-ray absorption spectroscopy, electron energy loss spectroscopy and density functional theory (DFT) calculations. These methods will help to investigate this material's underlying mechanisms, (iv) At the same time, water-splitting research is typically focused on alkaline conditions; it is also essential to explore the performance of these electrocatalysts in acidic mediums.

In light of our overview, it is clear that the LDH-MXene hybrid is regarded as the most promising electrocatalyst for water splitting. Serious experimental and theoretical investigations are being pursued for their water-splitting applications. Even though there are some shortcomings, extensive research in the future will be able to improve the performance of the LDH-MXene hybrid for industrial water-splitting applications.

Acknowledgment

Prof. AS gratefully acknowledges the UGC, New Delhi for their financial support under the BSR Mid-Career Award Scheme (No. F.19- 214/2018).

Conflict of Interest

There is no conflict of interest.

Supporting Information

Not applicable.

References

[1] P. De Luna, C. Hahn, D. Higgins, S. A. Jaffer, T. F. Jaramillo, E. H. Sargent, What would it take for renewably powered electrosynthesis to displace petrochemical processes? *Science*, 2019, **364**, eaav3506, doi: 10.1126/science.aav3506.

[2] J. Yu, T. A. Le, N. Q. Tran, H. Lee, Earth-abundant transition-metal-based bifunctional electrocatalysts for overall water splitting in alkaline media, *Chemistry - A European Journal*, 2020, **26**, 6423-6436, doi: 10.1002/chem.202000209.

[3] R. M. Bullock, J. G. Chen, L. Gagliardi, P. J. Chirik, O. K. Farha, C. H. Hendon, C. W. Jones, J. A. Keith, J. Klosin, S. D. Minteer, R. H. Morris, A. T. Radosevich, T. B. Rauchfuss, N. A.

Strotman, A. Vojvodic, T. R. Ward, J. Y. Yang, Y. Surendranath, Using nature's blueprint to expand catalysis with Earth-abundant metals, *Science*, 2020, **369**, eabc3183, doi: 10.1126/science.abc3183.
[4] Z. W. Seh, J. Kibsgaard, C. F. Dickens, I. Chorkendorff, J. K. Nørskov, T. F. Jaramillo, Combining theory and experiment in electrocatalysis: insights into materials design, *Science*, 2017, **355**, eaad4998, doi: 10.1126/science.aad4998.
[5] L. Dai, Y. Xue, L. Qu, H.-J. Choi, J.-B. Baek, Metal-free catalysts for oxygen reduction reaction, *Chemical Reviews*, 2015, **115**, 4823-4892, doi: 10.1021/cr5003563.
[6] A. Vasileff, Y. Zheng, S. Z. Qiao, Carbon solving carbon's problems: recent progress of nanostructured carbon-based catalysts for the electrochemical reduction of CO_2, *Advanced Energy Materials*, 2017, **7**, 1700759, doi: 10.1002/aenm.201700759.
[7] C. Forano, U. Costantino, V. Prévot, C. T. Gueho, Layered double hydroxides (LDH). Developments in Clay Science. Amsterdam: Elsevier, 2013, 745-782, doi: 10.1016/b978-0-08-098258-8.00025-0.
[8] Y. Wen, Z. Wei, J. Liu, R. Li, P. Wang, B. Zhou, X. Zhang, J. Li, Z. Li, Synergistic cerium doping and MXene coupling in layered double hydroxides as efficient electrocatalysts for oxygen evolution, *Journal of Energy Chemistry*, 2021, **52**, 412-420, doi: 10.1016/j.jechem.2020.04.009.
[9] F. L. Theiss, G. A. Ayoko, R. L. Frost, ChemInform abstract: synthesis of layered double hydroxides containing Mg^{2+}, Zn^{2+}, Ca^{2+} and Al^{3+} layer cations by Co-precipitation methods - A review, *ChemInform*, 2016, **47**, no, doi: 10.1002/chin.201633204.
[10] G. Zhao, J. Zou, X. Chen, J. Yu, F. Jiao, Layered double hydroxides materials for photo(electro-) catalytic applications, *Chemical Engineering Journal*, 2020, **397**, 125407, doi: 10.1016/j.cej.2020.125407.
[11] Y. Wang, D. Yan, S. El Hankari, Y. Zou, S. Wang, Recent progress on layered double hydroxides and their derivatives for electrocatalytic water splitting, *Advanced Science*, 2018, **5**, 1800064, doi: 10.1002/advs.201800064.
[12] G. M. Tomboc, J. Kim, Y. Wang, Y. Son, J. Li, J. Y. Kim, K. Lee, Hybrid layered double hydroxides as multifunctional nanomaterials for overall water splitting and supercapacitor applications, *Journal of Materials Chemistry A*, 2021, **9**, 4528-4557, doi: 10.1039/d0ta11606h.
[13] S. Kesavan Pillai, P. Kleyi, M. de Beer, P. Mudaly, Layered double hydroxides: an advanced encapsulation and delivery system for cosmetic ingredients-an overview, *Applied Clay Science*, 2020, **199**, 105868, doi: 10.1016/j.clay.2020.105868.
[14] X. Long, S. Xiao, Z. Wang, X. Zheng, S. Yang, Co intake mediated formation of ultrathin nanosheets of transition metal LDH—an advanced electrocatalyst for oxygen evolution reaction, *Chemical Communications*, 2015, **51**, 1120-1123, doi: 10.1039/c4cc08856e.
[15] Haixia, Liu, The effects of Al substitution and partial dissolution on ultrathin NiFeAl trinary layered double hydroxide nanosheets for oxygen evolution reaction in alkaline solution, *Nano Energy*, 2017, **35**, 350-357, doi: 10.1016/j.nanoen.2017.04.011.
[16] R. Liu, Y. Wang, D. Liu, Y. Zou, S. Wang, Water-plasma-enabled exfoliation of ultrathin layered double hydroxide nanosheets with multivacancies for water oxidation, *Advanced Materials*, 2017, **29**, 1701546, doi: 10.1002/adma.201701546.
[17] Yuanhao, Tang, Activating the hydrogen evolution and overall water splitting performance of NiFe LDH by cation doping and plasma reduction, *Applied Catalysis B: Environmental*, 2020, **266**, 118627, doi: 10.1016/j.apcatb.2020.118627.
[18] X. Zhang, Y. Zhao, Y. Zhao, R. Shi, G. I. N. Waterhouse, T. Zhang, A simple synthetic strategy toward defect-rich porous monolayer NiFe-layered double hydroxide nanosheets for efficient electrocatalytic water oxidation, *Advanced Energy Materials*, 2019, **9**, 1900881, doi: 10.1002/aenm.201900881.
[19] D. Tichit, M. G. Álvarez, Layered double hydroxide/nanocarbon composites as heterogeneous catalysts: a review, *ChemEngineering*, 2022, **6**, 45, doi: 10.3390/chemengineering6040045.
[20] M. Gong, Y. Li, H. Wang, Y. Liang, J. Z. Wu, J. Zhou, J. Wang, T. Regier, F. Wei, H. Dai, An advanced Ni-Fe layered double hydroxide electrocatalyst for water oxidation, *Journal of the American Chemical Society*, 2013, **135**, 8452-8455, doi: 10.1021/ja4027715.
[21] F. Gong, M. Liu, S. Ye, L. Gong, G. Zeng, L. Xu, X. Zhang, Y. Zhang, L. Zhou, S. Fang, J. Liu, All-pH stable sandwich-structured $MoO_2/MoS_2/C$ hollow nanoreactors for enhanced electrochemical hydrogen evolution, *Advanced Functional Materials*, 2021, **31**, 2101715, doi: 10.1002/adfm.202101715.
[22] J. Wang, X. Wei, W. Song, X. Shi, X. Wang, W. Zhong, M. Wang, J. Ju, Y. Tang, Plasmonic enhancement in water splitting performance for NiFe layered double hydroxide-N10TC MXene heterojunction, *ChemSusChem*, 2021, **14**, 1948-1954, doi: 10.1002/cssc.202100043.
[23] J. Zhu, L. Hu, P. Zhao, L. Y. S. Lee, K.-Y. Wong, Recent advances in electrocatalytic hydrogen evolution using nanoparticles, *Chemical Reviews*, 2020, **120**, 851-918, doi: 10.1021/acs.chemrev.9b00248.
[24] D. P. Sahoo, K. K. Das, S. Mansingh, S. Sultana, K. Parida, Recent progress in first row transition metal Layered double hydroxide (LDH) based electrocatalysts towards water splitting: a review with insights on synthesis, *Coordination Chemistry Reviews*, 2022, **469**, 214666, doi: 10.1016/j.ccr.2022.214666.
[25] X.-P. Li, C. Huang, W.-K. Han, T. Ouyang, Z.-Q. Liu, Transition metal-based electrocatalysts for overall water splitting, *Chinese Chemical Letters*, 2021, **32**, 2597-2616, doi: 10.1016/j.cclet.2021.01.047.
[26] C. G. Morales-Guio, L.-A. Stern, X. Hu, Nanostructured hydrotreating catalysts for electrochemical hydrogen evolution, *Chemical Society Reviews*, 2014, **43**, 6555, doi: 10.1039/c3cs60468c.
[27] Y. Xu, K. Fan, Y. Zou, H. Fu, M. Dong, Y. Dou, Y. Wang, S. Chen, H. Yin, M. Al-Mamun, P. Liu, H. Zhao, Rational design of metal oxide catalysts for electrocatalytic water splitting,

Nanoscale, 2021, **13**, 20324-20353, doi: 10.1039/d1nr06285a.
[28] J. Zhao, J.-J. Zhang, Z.-Y. Li, X.-H. Bu, Recent progress on NiFe-based electrocatalysts for the oxygen evolution reaction, *Small*, 2020, **16**, 2003916, doi: 10.1002/smll.202003916.
[29] R. He, X. Huang, L. Feng, Recent progress in transition-metal sulfide catalyst regulation for improved oxygen evolution reaction, *Energy & Fuels*, 2022, **36**, 6675-6694, doi: 10.1021/acs.energyfuels.2c01429.
[30] H. Narayanan, B. Viswanathan, K. R. Krishnamurthy, H. Nair, Hydrogen from photo-electrocatalytic water splitting, Solar Hydrogen Production. Amsterdam: Elsevier, 2019, 419-486, doi: 10.1016/b978-0-12-814853-2.00012-6.
[31] M. Datt Bhatt, J. Y. Lee, Advancement of platinum (Pt)-free (non-Pt precious metals) and/or metal-free (non-precious-metals) electrocatalysts in energy applications: a review and perspectives, *Energy & Fuels*, 2020, **34**, 6634-6695, doi: 10.1021/acs.energyfuels.0c00953.
[32] C. Wang, H. Shang, H. Xu, Y. Du, Nanoboxes endow non-noble-metal-based electrocatalysts with high efficiency for overall water splitting, *Journal of Materials Chemistry A*, 2021, **9**, 857-874, doi: 10.1039/d0ta10596a.
[33] C. Wang, H. Shang, H. Xu, Y. Du, Nanoboxes endow non-noble-metal-based electrocatalysts with high efficiency for overall water splitting, *Journal of Materials Chemistry A*, 2021, **9**, 857-874, doi: 10.1039/d0ta10596a.
[34] X. Zou, Y. Zhang, Noble metal-free hydrogen evolution catalysts for water splitting, *Chemical Society Reviews*, 2015, **44**, 5148-5180, doi: 10.1039/c4cs00448e.
[35] S. Li, E. Li, X. An, X. Hao, Z. Jiang, G. Guan, Transition metal-based catalysts for electrochemical water splitting at high current density: current status and perspectives, *Nanoscale*, 2021, **13**, 12788-12817, doi: 10.1039/d1nr02592a.
[36] B. Xiong, L. Chen, J. Shi, Anion-containing noble-metal-free bifunctional electrocatalysts for overall water splitting, *ACS Catalysis*, 2018, **8**, 3688-3707, doi: 10.1021/acscatal.7b04286.
[37] K. Qu, Y. Zheng, Y. Jiao, X. Zhang, S. Dai, S.-Z. Qiao, Polydopamine-inspired, dual heteroatom-doped carbon nanotubes for highly efficient overall water splitting, *Advanced Energy Materials*, 2017, **7**, 1602068, doi: 10.1002/aenm.201602068.
[38] N.-T. Suen, S.-F. Hung, Q. Quan, N. Zhang, Y.-J. Xu, H. M. Chen, Electrocatalysis for the oxygen evolution reaction: recent development and future perspectives, *Chemical Society Reviews*, 2017, **46**, 337-365, doi: 10.1039/c6cs00328a.
[39] A. Vazhayil, L. Vazhayal, J. Thomas, S. Ashok C, N. Thomas, A comprehensive review on the recent developments in transition metal-based electrocatalysts for oxygen evolution reaction, *Applied Surface Science Advances*, 2021, **6**, 100184, doi: 10.1016/j.apsadv.2021.100184.
[40] D. Li, H. Liu, L. Feng, A review on advanced FeNi-based catalysts for water splitting reaction, *Energy & Fuels*, 2020, **34**, 13491-13522, doi: 10.1021/acs.energyfuels.0c03084.
[41] G. T. Burstein, A hundred years of Tafel's Equation: 1905-2005, *Corrosion Science*, 2005, **47**, 2858-2870, doi: 10.1016/j.corsci.2005.07.002.
[42] S. Anantharaj, S. R. Ede, K. Sakthikumar, K. Karthick, S. Mishra, S. Kundu, Recent trends and perspectives in electrochemical water splitting with an emphasis on sulfide, selenide, and phosphide catalysts of Fe, Co, and Ni: A review, *ACS Catalysis*, 2016, **6**, 8069-8097, doi: 10.1021/acscatal.6b02479.
[43] A. Karmakar, K. Karthick, S. S. Sankar, S. Kumaravel, R. Madhu, S. Kundu, A vast exploration of improvising synthetic strategies for enhancing the OER kinetics of LDH structures: a review, *Journal of Materials Chemistry A*, 2021, **9**, 1314-1352, doi: 10.1039/d0ta09788h.
[44] Y. Yan, B. Y. Xia, B. Zhao, X. Wang, A review on noble-metal-free bifunctional heterogeneous catalysts for overall electrochemical water splitting, *Journal of Materials Chemistry A*, 2016, **4**, 17587-17603, doi: 10.1039/c6ta08075h.
[45] S. Wang, A. Lu, C.-J. Zhong, Hydrogen production from water electrolysis: role of catalysts, Nano Convergence, 2021, **8**, 1-23, doi: 10.1186/s40580-021-00254-x.
[46] S. Anantharaj, P. E. Karthik, S. Kundu, Self-assembled IrO2nanoparticles on a DNA scaffold with enhanced catalytic and oxygen evolution reaction (OER) activities, *Journal of Materials Chemistry A*, 2015, **3**, 24463-24478, doi: 10.1039/c5ta07075a.
[47] S. Anantharaj, M. Jayachandran, S. Kundu, Unprotected and interconnected Ru0 nano-chain networks: advantages of unprotected surfaces in catalysis and electrocatalysis, *Chemical Science*, 2016, **7**, 3188-3205, doi: 10.1039/c5sc04714e.
[48] S. Anantharaj, P. E. Karthik, B. Subramanian, S. Kundu, Pt nanoparticle anchored molecular self-assemblies of DNA: an extremely stable and efficient HER electrocatalyst with ultralow Pt content, *ACS Catalysis*, 2016, **6**, 4660-4672, doi: 10.1021/acscatal.6b00965.
[49] S. Anantharaj, P. E. Karthik, S. Kundu, Petal-like hierarchical array of ultrathin $Ni(OH)_2$ nanosheets decorated with Ni(OH)2 nanoburls: a highly efficient OER electrocatalyst, *Catalysis Science & Technology*, 2017, **7**, 882-893, doi: 10.1039/c6cy02282k.
[50] X.-Y. Zhang, J.-Y. Xie, Y. Ma, B. Dong, C.-G. Liu, Y.-M. Chai, An overview of the active sites in transition metal electrocatalysts and their practical activity for hydrogen evolution reaction, *Chemical Engineering Journal*, 2022, **430**, 132312, doi: 10.1016/j.cej.2021.132312.
[51] M. Tahir, L. Pan, F. Idrees, X. Zhang, L. Wang, J.-J. Zou, Z. L. Wang, Electrocatalytic oxygen evolution reaction for energy conversion and storage: a comprehensive review, *Nano Energy*, 2017, **37**, 136-157, doi: 10.1016/j.nanoen.2017.05.022.
[52] F. Zeng, C. Mebrahtu, L. Liao, A. K. Beine, R. Palkovits, Stability and deactivation of OER electrocatalysts: a review, *Journal of Energy Chemistry*, 2022, **69**, 301-329, doi: 10.1016/j.jechem.2022.01.025.
[53] Y. Shi, B. Zhang, Recent advances in transition metal phosphide nanomaterials: synthesis and applications in hydrogen evolution reaction, *Chemical Society Reviews*, 2016, **45**, 1529-1541, doi: 10.1039/c5cs00434a.
[54] S.-X. Guo, Y. Liu, A. M. Bond, J. Zhang, P. Esakki Karthik, I. Maheshwaran, S. Senthil Kumar, K. L. N. Phani, Facile

electrochemical co-deposition of a graphene-cobalt nanocomposite for highly efficient water oxidation in alkaline media: direct detection of underlying electron transfer reactions under catalytic turnover conditions, *Phys Chem Chem Phys*, 2014, **16**, 19035-19045, doi: 10.1039/c4cp01608d.

[55] M. Görlin, P. Chernev, J. Ferreira de Araújo, T. Reier, S. Dresp, B. Paul, R. Krähnert, H. Dau, P. Strasser, Oxygen evolution reaction dynamics, faradaic charge efficiency, and the active metal redox states of Ni-Fe oxide water splitting electrocatalysts, *Journal of the American Chemical Society*, 2016, **138**, 5603-5614, doi: 10.1021/jacs.6b00332.

[56] Y.-H. Fang, Z.-P. Liu, Tafel kinetics of electrocatalytic reactions: from experiment to first-principles, *ACS Catalysis*, 2014, **4**, 4364-4376, doi: 10.1021/cs501312v.

[57] D. Tian, S. R. Denny, K. Li, H. Wang, S. Kattel, J. G. Chen, Density functional theory studies of transition metal carbides and nitrides as electrocatalysts, *Chemical Society Reviews*, 2021, **50**, 12338-12376, doi: 10.1039/d1cs00590a.

[58] M. Benchakar, T. Bilyk, C. Garnero, L. Loupias, C. Morais, J. Pacaud, C. Canaff, P. Chartier, S. Morisset, N. Guignard, V. Mauchamp, S. Célérier, A. Habrioux, MXene supported cobalt layered double hydroxide nanocrystals: facile synthesis route for a synergistic oxygen evolution reaction electrocatalyst, *Advanced Materials Interfaces*, 2019, **6**, 1901328, doi: 10.1002/admi.201901328.

[59] L. Deng, K. Zhang, D. Shi, S. Liu, D. Xu, Y. Shao, J. Shen, Y. Wu, X. Hao, Rational design of Schottky heterojunction with modulating surface electron density for high-performance overall water splitting, *Applied Catalysis B: Environmental*, 2021, **299**, 120660, doi: 10.1016/j.apcatb.2021.120660.

[60] C. Hao, Y. Wu, Y. An, B. Cui, J. Lin, X. Li, D. Wang, M. Jiang, Z. Cheng, S. Hu, Interface-coupling of CoFe-LDH on MXene as high-performance oxygen evolution catalyst, *Materials Today Energy*, 2019, **12**, 453-462, doi: 10.1016/j.mtener.2019.04.009.

[61] A. Grimaud, O. Diaz-Morales, B. Han, W. T. Hong, Y.-L. Lee, L. Giordano, K. A. Stoerzinger, M. T. M. Koper, Y. Shao-Horn, Activating lattice oxygen redox reactions in metal oxides to catalyse oxygen evolution, *Nature Chemistry*, 2017, **9**, 457-465, doi: 10.1038/nchem.2695.

[62] E. L. Crepaldi, P. C. Pavan, J. B. Valim, Comparative study of the coprecipitation methods for the preparation of Layered Double Hydroxides, *Journal of the Brazilian Chemical Society*, 2000, **11**, 64-70, doi: 10.1590/s0103-50532000000100012.

[63] M. C. Gastuche, G. Brown, M. M. Mortland, Mixed magnesium-aluminiun hydroxides. I. Preparation and characterization of compounds formed in dialysed systems, *Clay Minerals*, 1967, **7**, 177-192, doi: 10.1180/claymin.1967.007.2.05.

[64] S. Miyata, The Syntheses of Hydrotalcite-Like Compounds and Their Structures and Physico-Chemical Properties—I: the Systems Mg^{2+}-Al^{3+}-NO^{-3}, Mg^{2+}-Al^{3+}-Cl^{-}, Mg^{2+}-Al^{3+}-ClO^{-4}, Ni^{2+}-Al^{3+}-Cl^{-} and Zn^{2+}-Al^{3+}-Cl^{-}, *Clays and Clay Minerals*, 1975, **23**, 369–375, doi: 10.1346/CCMN.1975.0230508.

[65] S. Miyata, Physico-chemical properties of synthetic hydrotalcites in relation to composition, *Clays and Clay Minerals*, 1980, **28**, 50-56, doi: 10.1346/CCMN.1980.0280107.

[66] Z. P. Xu, G. Q. M. Lu, Hydrothermal synthesis of layered double hydroxides (LDHs) from mixed MgO and Al2O3: LDH formation mechanism, *Chemistry of Materials*, 2005, **17**, 1055-1062, doi: 10.1021/cm048085g.

[67] R. P. Bontchev, S. Liu, J. L. Krumhansl, J. Voigt, T. M. Nenoff, Synthesis, characterization, and ion exchange properties of hydrotalcite $Mg_6Al_2(OH)_{16}(a)_x(A')_{2-x}\cdot 4H_2O$ (A, A'= Cl-, Br-, I-, and NO^{3-}, $2 \geq x \geq 0$) derivatives, *Chemistry of Materials*, 2003, **15**, 3669-3675, doi: 10.1021/cm034231r.

[68], Roelofs, Lensveld, V. Dillen, D. Jong, On the structure of activated hydrotalcites as solid base catalysts for liquid-phase aldol condensation, *Journal of Catalysis*, 2001, **203**, 184-191, doi: 10.1006/jcat.2001.3295.

[69] W. N. Budhysutanto, H. J. M. Kramer, D. van Agterveld, A. G. Talma, P. J. Jansens, Pre-treatment of raw materials for the hydrothermal synthesis of hydrotalcite-like compounds, *Chemical Engineering Research and Design*, 2010, **88**, 1445-1449, doi: 10.1016/j.cherd.2009.10.010.

[70] F. J. W. J. Labuschagné, A. Wiid, H. P. Venter, B. R. Gevers, A. Leuteritz, Green synthesis of hydrotalcite from untreated magnesium oxide and aluminum hydroxide, *Green Chemistry Letters and Reviews*, 2018, **11**, 18-28, doi: 10.1080/17518253.2018.1426791.

[71] L. Liao, N. Zhao, Z. Xia, Hydrothermal synthesis of Mg-Al layered double hydroxides (LDHs) from natural brucite and Al(OH)3, *Materials Research Bulletin*, 2012, **47**, 3897-3901, doi: 10.1016/j.materresbull.2012.07.007.

[72] J. Prince, A. Montoya, G. Ferrat, J. S. Valente, Proposed general Sol–gel method to prepare multimetallic layered double hydroxides: synthesis, characterization, and envisaged application, *Chemistry of Materials*, 2009, **21**, 5826-5835, doi: 10.1021/cm902741c.

[73] A. Mahmoud, Ahmed, A systematic review of layered double hydroxide-based materials for environmental remediation of heavy metals and dye pollutants, *Inorganic Chemistry Communications*, 2023, **148**, 110325, doi: 10.1016/j.inoche.2022.110325.

[74] S. T. Mahmud, M. M. Hasan, S. Bain, S. T. Rahman, M. Rhaman, M. M. Hossain, M. Ordu, Multilayer MXene heterostructures and nanohybrids for multifunctional applications: a review, *ACS Materials Letters*, 2022, **4**, 1174-1206, doi: 10.1021/acsmaterialslett.2c00175.

[75] A. Liu, X. Liang, X. Ren, W. Guan, M. Gao, Y. Yang, Q. Yang, L. Gao, Y. Li, T. Ma, Recent progress in MXene-based materials: potential high-performance electrocatalysts, *Advanced Functional Materials*, 2020, **30**, 2003437, doi: 10.1002/adfm.202003437.

[76] H. Yu, Y. Wang, Y. Jing, J. Ma, C.-F. Du, Q. Yan, Surface modified MXene-based nanocomposites for electrochemical energy conversion and storage, *Small*, 2019, **15**, 1901503, doi: 10.1002/smll.201901503.

[77] X. Li, Z. Zhang, Q. Xiang, R. Chen, D. Wu, G. Li, L. Wang, A three-dimensional flower-like NiCo-layered double hydroxide grown on nickel foam with an MXene coating for enhanced oxygen evolution reaction electrocatalysis, *RSC Advances*, 2021, **11**, 12392-12397, doi: 10.1039/d1ra01368h.
[78] Y. Liu, L. Bai, T. Li, H. Liu, X. Wang, L. Zhang, X. Hao, C. He, S. Guo, MXene-supported NiMn-LDHs as efficient electrocatalysts towards enhanced oxygen evolution reactions, *Materials Advances*, 2022, **3**, 4359-4368, doi: 10.1039/d2ma00302c.
[79] G. Chen, T. Wang, J. Zhang, P. Liu, H. Sun, X. Zhuang, M. Chen, X. Feng, Accelerated hydrogen evolution kinetics on NiFe-layered double hydroxide electrocatalysts by tailoring water dissociation active sites, *Advanced Materials*, 2018, **30**, 1706279, doi: 10.1002/adma.201706279.
[80] J. Ping, Y. Wang, Q. Lu, B. Chen, J. Chen, Y. Huang, Q. Ma, C. Tan, J. Yang, X. Cao, Z. Wang, J. Wu, Y. Ying, H. Zhang, Self-assembly of single-layer CoAl-layered double hydroxide nanosheets on 3D graphene network used as highly efficient electrocatalyst for oxygen evolution reaction, *Advanced Materials*, 2016, **28**, 7640-7645, doi: 10.1002/adma.201601019.
[81] B. Shen, H. Huang, Y. Jiang, Y. Xue, H. He, 3D interweaving MXene-graphene network-confined Ni-Fe layered double hydroxide nanosheets for enhanced hydrogen evolution, *Electrochimica Acta*, 2022, **407**, 139913, doi: 10.1016/j.electacta.2022.139913.
[82] Z. Zhu, C. Xu, Y. Wang, L. Wang, Z. Chang, Z. Fang, X. Liu, J. Cheng, The high performance NiFe layered double hydroxides@ Ti_3C_2Tx/reduced graphene oxide hybrid catalyst for oxygen evolution reaction, *Journal of Alloys and Compounds*, 2022, **894**, 162393, doi: 10.1016/j.jallcom.2021.162393.
[83] Z. Li, X. Wang, J. Ren, H. Wang, NiFe LDH/Ti3C2Tx/nickel foam as a binder-free electrode with enhanced oxygen evolution reaction performance, *International Journal of Hydrogen Energy*, 2022, **47**, 3886-3892, doi: 10.1016/j.ijhydene.2021.11.048.
[84] L. Hu, R. Xiao, X. Wang, X. Wang, C. Wang, J. Wen, W. Gu, C. Zhu, MXene-induced electronic optimization of metal-organic framework-derived CoFe LDH nanosheet arrays for efficient oxygen evolution, *Applied Catalysis B: Environmental*, 2021, **298**, 120599, doi: 10.1016/j.apcatb.2021.120599.
[85] Mengzhou, Yu, Boosting electrocatalytic oxygen evolution by synergistically coupling layered double hydroxide with MXene, *Nano Energy*, 2018, **44**, 181-190, doi: 10.1016/j.nanoen.2017.12.003.
[86] M. Li, R. Sun, Y. Li, J. Jiang, W. Xu, H. Cong, S. Han, The 3D porous "celosia" heterogeneous interface engineering of layered double hydroxide and P-doped molybdenum oxide on MXene promotes overall water-splitting, *Chemical Engineering Journal*, 2022, **431**, 133941, doi: 10.1016/j.cej.2021.133941.
[87] Mengzhou, Yu, La-doped NiFe-LDH coupled with hierarchical vertically aligned MXene frameworks for efficient overall water splitting, *Journal of Energy Chemistry*, 2022, **70**, 472-479, doi: 10.1016/j.jechem.2022.02.044.
[88] G.L. Li, S. Cao, Z.F. Lu, X. Wang, Y. Yan, C. Hao, FePc nanoclusters modified NiCo layered double hydroxides in parallel with Ti_3C_2 MXene as a highly efficient and durable bifunctional oxygen electrocatalyst for zinc-air batteries, *Applied Surface Science*, 2022, **591**, 153142, doi: 10.1016/j.apsusc.2022.153142.
[89] M. Tian, Y. Jiang, H. Tong, Y. Xu, L. Xia, MXene-supported FeCo-LDHs as highly efficient catalysts for enhanced electrocatalytic oxygen evolution reaction, *ChemNanoMat*, 2020, **6**, 154-159, doi: 10.1002/cnma.201900613.
[90] Y. Chen, H. Yao, F. Kong, H. Tian, G. Meng, S. Wang, X. Mao, X. Cui, X. Hou, J. Shi, V2C MXene synergistically coupling FeNi LDH nanosheets for boosting oxygen evolution reaction, *Applied Catalysis B: Environmental*, 2021, **297**, 120474, doi: 10.1016/j.apcatb.2021.120474.
[91] M. Yu, S. Zhou, Z. Wang, J. Zhao, J. Qiu, Boosting electrocatalytic oxygen evolution by synergistically coupling layered double hydroxide with MXene, *Nano Energy*, 2018, **44**, 181-190, doi: 10.1016/j.nanoen.2017.12.003.
[92] M. Faraji, N. Arianpouya, NiCoFe-layered double hydroxides/MXene/N-doped carbon nanotube composite as a high-performance bifunctional catalyst for oxygen electrocatalytic reactions in metal-air batteries, *Journal of Electroanalytical Chemistry*, 2021, **901**, 115797, doi: 10.1016/j.jelechem.2021.115797.

Author Information

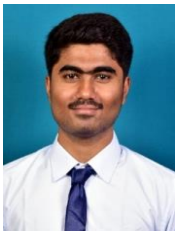

Anandajayarajan Udayakumar *received his B.Tech. in Chemical and Electrochemical Engineering from CSIR- Karaikudi in 2020 and his M. Tech in Nanoscience and Technology at Pondicherry University in 2022. He is currently pursuing his Ph.D. in Mechanical Engineering at University of Illinois Chicago. His current research interests include the development of electrocatalysts for water splitting, electrodes for Lithium - Carbon dioxide battery.*

Preethi Dhandapani *received her B. Tech in Chemical Engineering from Pondicherry Engineering College in 2017 and her M. Tech in Nanoscience and Technology at Pondicherry University in 2019. She is currently pursuing her Ph.D. in Nanoscience and Technology at Pondicherry University under the supervision of Prof. Subramania Angaiah, in the development of hybrid electrode materials for supercapacitors and water splitting.*

Senthilkumar Ramasamy *is currently working as an Assistant Professor at Amrita Vishwa Vidyapeetham University, Coimbatore campus. He received his Ph.D. degree in Chemical Engineering & Materials Science from Amrita Vishwa Vidyapeetham University, Coimbatore, in 2020. His current*

research interests include Dye-sensitized solar cells, Perovskite solar cells, Photocatalysis, and Nanomaterials for Energy and Environmental remediation.

Subramania Angaiah *is working as a Professor at the Centre for Nanoscience and Technology, Pondicherry University, India. He obtained his Ph.D. degree from Alagappa University & CSIR-CECRI and his Postdoctoral training from the Korean Institute of Science and Technology (KIST), Seoul, South Korea. His current research interests include the development of Metal-ion batteries, Supercapacitors, DSSC, QDSSC, PSC, Bio-sensors, Electro-catalysis for Water splitting, Secondary metal recovery from waste, Corrosion studies, etc.*

